Presupernova collapse models with improved weak-interaction rates

A. Heger[1], K. Langanke[2], G. Martínez-Pinedo[2], and S.E. Woosley[1]
[1] *UCO/Lick Observatory, University of California, Santa Cruz CA 95064, USA*
[2] *Institut for Fysik og Astronomi, Århus Universitet, DK-8000 Århus C, Denmark*
(February 1, 2008)

Improved values for stellar weak interaction rates have been recently calculated based upon a large shell model diagonalization. Using these new rates (for both beta decay and electron capture), we have examined the presupernova evolution of massive stars in the range 15–40 $M_\odot$. Comparing our new models with a standard set of presupernova models by Woosley and Weaver, we find significantly larger values for the electron-to-baryon ratio Y_e at the onset of collapse and iron core masses reduced by approximately 0.1 $M_\odot$. The inclusion of beta-decay accounts for roughly half of the revisions, while the other half is a consequence of the improved nuclear physics. These changes will have important consequences for nucleosynthesis and the supernova explosion mechanism.

PACS numbers: 26.50.+x, 97.60.Bw, 97.10.Cv

arXiv:astro-ph/0007412v1 27 Jul 2000

The late stages of massive stellar evolution are strongly influenced by weak interactions which act to determine the core entropy and electron-to-baryon ratio, Y_e, of the presupernova star. Electron capture reduces the number of electrons available for pressure support, while beta decay acts in the opposite direction. Both processes generate neutrinos which, for densities $\rho \lesssim 10^{11}$ g/cm^3, escape the star carrying away energy and entropy from the core.

Electron capture and beta decay during the final evolution of a massive star are dominated by Fermi and Gamow-Teller (GT) transitions. While the treatment of Fermi transitions (important only in beta decays) is straightforward, a correct description of the GT transitions is a difficult problem in nuclear structure. In their pioneering work on the subject Fuller, Fowler and Newman (FFN) [1] estimated electron-capture rates assuming a single GT resonance. The properties of this resonance were derived on the basis of the independent particle model, supplemented by Fermi contributions and experimental data for low-lying transitions, whenever available. These authors also noted the importance of the 'backresonances' for beta decay. These are excited states in the decaying nucleus which are connected by strong GT transitions to low-lying states in the daughter nucleus and, by thermal population and with increased phase space, can significantly contribute to the stellar beta decay rates.

Recent experimental data shows that the GT distributions in nuclei are quenched, compared to the independent particle model value, and strongly fragmented over many states in the daughter nucleus. Both effects are caused by residual interaction among the valence nucleons and an accurate description of these correlations is essential for a reliable evaluation of the stellar weak interaction rates due to the strong phase space energy dependence, particularly of the stellar electron capture rates. The shell model is the only known tool to reliably describe GT distributions in nuclei [2]. Its application to iron mass nuclei in the middle of the pf-shell as required in the presupernova collapse, however, has long been inhibited due to the extremely large model space dimensions involved. After significant progress in shell-model programming [3] and hardware development the situation has changed very recently and in Ref. [4] it has been demonstrated that state-of-the-art diagonalization studies, typically involving a few 10 million configurations, are indeed able to reproduce all relevant ingredients ($GT_\pm$ strength distributions for changing protons (neutrons) into neutrons (protons), level spectra and half-lives) and hence have the predictive power to reliably calculate stellar weak interaction rates. This program has recently been finished and stellar weak-interaction rates for nuclei with A = 45–65 have been calculated based on the shell-model results, supplemented by experimental data, wherever available. The shell-model rates have been discussed and validated in [5]. It has been found that for pf-shell nuclei the shell-model electron-capture rates are smaller than the FFN rates by, on average, an order of magnitude, for the reasons explained in [5]. The situation is different for the beta decay as the shell model and FFN rates are of the same magnitude for the most relevant nuclei to be identified below.

To study the influence of the shell model rates on presupernova models we have repeated the calculations of Woosley and Weaver [6] (henceforth WW) keeping all the stellar physics, except for weak rates, as close to the original studies as possible. The present calculations have incorporated the new shell-model weak interaction rates (including electron capture, positron emission, and beta decay) for nuclei with mass numbers A = 45–65, supplemented by rates from Oda *et al.* [7] for lighter nuclei. In practice, the weak rates for these lighter nuclei were not very important for determining the presupernova structure, but only dominate prior to silicon burning. We also note that, for *sd*-shell nuclei with $A = 17 - 39$, the FFN rates agree rather well with the shell model rates previously determined by Oda *et al.* [7].

The earlier calculations of WW, to which we compare, used the FFN rates for electron capture and an older set of beta-decay rates taken from [8] and [9]. Shortly after the models of WW were calculated, it was recognized

that these older beta-decay rates were inadequate and that use of the larger values from FFN would appreciably alter the results [10]. These are the first models of the WW variety to incorporate realistic beta-decay rates and electron-capture rates in a complete stellar model, even though beta decays were included in some other models of massive stellar evolution [11]. In a separate paper [12], we will present the comparison of models that use the full FFN rate set and the new rate set, and in a future paper we will examine the evolution of stars of other mass and metallicity.

Fig. 1 shows the late evolution, following core oxygen burning, of the central temperature and density in $15\,M_\odot$ and $25\,M_\odot$ stars as well as the central value of the electron-to-baryon ratio, Y_e. Time is measured here backwards from the time of iron core collapse, which is arbitrarily t = 0. Silicon burning ignites with a mild "flash" and the core becomes convective and expands. For the $25\,M_\odot$ star the temperature and density trajectories in the new and old models are similar, but the calculations with shell model rates have significantly larger values of Y_e. This difference persists throughout the iron core, not just at its center. Larger values of Y_e also result in the $15\,M_\odot$ star, but there even the density and temperature structures of the presupernova star are appreciably altered.

To understand the origin of these differences, we will now explore the role of the weak-interaction rates in greater detail. Weak processes become particularly important in reducing Y_e below 0.50 after oxygen depletion ($\sim 10^7$ s and 10^6 s before core collapse for the $15\,M_\odot$ and $25\,M_\odot$ stars, respectively) and Y_e begins a decline that becomes precipitous during silicon burning. Initially electron capture occurs much more rapidly than beta decay. Since the shell model rates are generally smaller than the FFN electron capture rates, the initial reduction of Y_e is smaller in the new models. The reduction is less pronounced during silicon shell burning both because the evolution time scale becomes quite short and because nuclei near the valley of beta-stability, with smaller weak-interaction rates, have already been produced (from a composition that initially had $N = Z$). During this period the core matter is composed of nuclei with $A < 65$ which are carried in the calculation.

An important feature of the new models is that beta decay becomes temporarily competitive with electron capture after silicon depletion in the core and during silicon shell burning. That this would occur was foreseen by [10] on the basis of one-zone models. Here we see it occurring in a complete stellar model. Moreover, the new electron capture rates are smaller than FFN and thus offer less resistance to beta decay. Dynamic weak equilibrium, in the sense described by [10], thus occurs at larger values of Y_e. Interestingly, by the time the iron core is actually collapsing, weak equilibrium no longer exists. The increase in density closes the phase space for beta decay and electron capture again predominates by a large factor. It is this special characteristic of "presupernova models" that lead some researchers in the past to miss the importance of beta decay during a transient stage an hour or so *prior to collapse*.

While dynamic weak equilibrium is achieved in the $15\,M_\odot$ model, with the new rates, it is not in the $25\,M_\odot$, though beta-decay still offers a non-negligible resistance to electron capture even there. This is in part due to the shorter time scale of silicon shell burning in the more massive star and also the larger value of Y_e in the cores of stars with higher entropies (Fig. 1).

The presence of an important beta-decay contribution has two effects. Obviously it counteracts the reduction of Y_e in the core, but equally important, beta decays are an additional neutrino source and thus add to the cooling of the core and a reduction in entropy [10]. This cooling can be quite efficient, as often the average neutrino energy in the involved beta decays is larger than for the competing electron captures. As a consequence the new models have significant lower core temperatures than the WW models after silicon burning, which is particularly pronounced for the $15\,M_\odot$ star. During the contraction stage electron capture is again more important than beta decays, associated with the increased electron Fermi energy. Although the shell model rates are individually smaller than the FFN electron capture rates, the effective electron capture rate is larger in the new models as the evolution now proceeds along a trajectory with larger Y_e values involving nuclei with smaller Q-values thus making electron capture energetically easier.

In summary, the shell model weak interaction rates result in significantly larger Y_e values during the presupernova evolution of a 15 and $25\,M_\odot$ star than calculated by WW. Part - about half - of the change is due to including beta-decay and the other half is due to slower rates for electron capture. Fig. 2 shows that this is a general finding for all stars in the mass range 11–$40\,M_\odot$. The central values of Y_e at the onset of core collapse are increased by 0.01–0.015. This is a significant effect. We note that the new models also result in lower core entropies for stars with $M \lesssim 20\,M_\odot$. The larger core Y_e values and the lower entropies suggest that these stars will have a larger homologous core than currently assumed. For $M \gtrsim 20\,M_\odot$, the new models actually have a slightly larger entropy. Thus one might expect that increased electron capture rate on (the more abundant) free protons will partly counteract the increase in Y_e values during the subsequent core collapse phase. In general, core collapse calculations with detailed neutrino transport are required before definite conclusions about the explosion mechanism can be drawn. We will provide our models to those wishing to attempt such calculations.

Another important property for the core collapse is the size of the iron core, which we define as the mass interior to the point where the composition becomes at

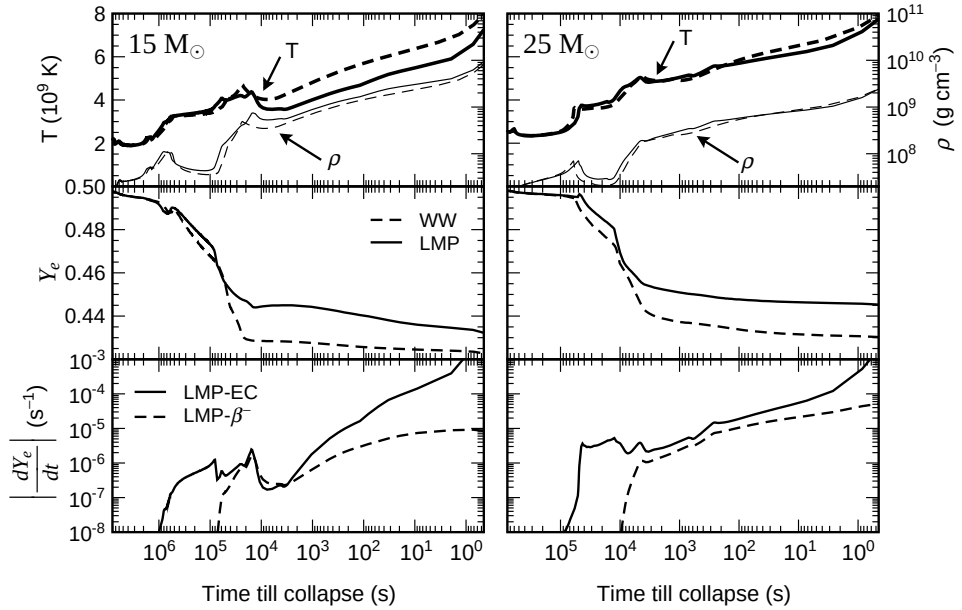

FIG. 1. Comparison of the time evolution of key quantities at the center of a $15\,M_\odot$ (left) and $25\,M_\odot$ (right) star between the models by Woosley & Weaver models (WW, dashed) [6] and the present ones using the shell model weak interaction rates (LMP, full lines). The upper panels show the temperature (thick lines) and density (thin lines), the middle panels show the electron-to-baryon ratio, Y_e, and the lower panels show the time-derivative of Y_e due to electron capture and beta decay for the models using the LMP rates. As reference points, in the $15\,M_\odot$ ($25\,M_\odot$) star central silicon burning ignites at 7×10^5 s (5.6×10^4 s), terminates at 6.6×10^4 s (10^4 s), silicon shell burning starts at 3.2×10^4 s (4.7×10^3 s) and core contraction set in at $t\sim280$ s (~230 s) before core collapse. Note that the dY_e/dt shown in the lower panels includes only the contribution of weak interaction processes to the total change of the central Y_e; during central silicon burning convection mixes down matter with higher Y_e from layers above [12].

least 50 % of iron group elements ($A \geq 48$). As is shown in Fig. 2, the iron core masses are generally smaller in the new models. The effect is larger for stars more massive than $20\,M_\odot$, while for the most common supernovae ($M \lesssim 20\,M_\odot$) the reduction is about $0.05\,M_\odot$. This reduction appears to be counterintuitive at first glance with respect to the slower electron capture rates in the new models. It is, however, related to changes in the entropy profile during silicon shell burning which reduces the growth of the iron core just prior to collapse [12]. Clearly, though we have, for reasons of space concentrated upon central values, it is the entire distribution of entropy and Y_e in the stellar interior that determines its final evolution.

Confidence in the shell model rates stems from the recent measurements of GT distributions in iron mass nuclei which are all well reproduced by the shell model calculations [4]. However, the energy resolutions of these pioneering (n,p) charge-exchange studies performed at TRIUMF has been rather limited ($\sim$ 1–1.5 MeV) and they have been performed for stable nuclei only. These limitations are likely to be overcome in the near future as measurements with charge-exchange reactions like (d, ^{2}He), (t, ^{3}He) promise data with an order of magnitude improved resolution. Furthermore, after radioactive ion beam facilities will become operational it will be possible by inverse techniques also to determine the GT distributions for unstable nuclei. Of course, laboratory experiments cannot measure directly the relevant stellar rates as these involve, for example, electron capture or beta decays from excited states. Nevertheless, high-resolution charge-exchange or beta-decay experiments are important for two reasons: First, they are stringent constraints for the nuclear models and their predictive powers. Second, such experiments can determine the energy positions of the daughter states for the GT transitions which can then be used directly in the determination of the rates.

To guide such experiments we have attempted to identify the most important nuclei for electron-capture and beta decay during the final stages of stellar evolution. The relevant quantity is the product of abundance of the nuclear species in the core composition and electron capture rate (or beta decay rate). Table I lists the most important nuclei at selected points during the final evolution of our $15\,M_\odot$ and $25\,M_\odot$ stars. Since the Y_e values are significantly larger in the new models, the important flows now involve nuclei much closer to stability so that several of the most important electron capturing nuclei (e.g., ^{54,56,58}Fe, ^{55}Mn, ^{53}Cr) are stable. Beta decay, on

TABLE I. Most important nuclei for electron capture and beta decay at selected points (characterized by temperature T, density ρ and electron-to-baryon ratio Y_e) during the final evolution of a 15 $M_\odot$ and 25 $M_\odot$ stars. The total electron capture λ_{ec} and beta decay $\lambda_{\beta-}$ rates are listed as well as the 3 dominating nuclei; the number in parentheses defines their percentage to the respective rates.

T (K)	ρ (g cm^{-3})	Y_e	λ_{ec} (s^{-1})	electron capture			$\lambda_{\beta-}$ (s^{-1})	beta decay		
				15 $M_\odot$						
3.39×10^9	4.50×10^7	0.480	5.17×10^{-7}	^{54}Fe (29)	^{55}Fe (25)	^{53}Mn (11)	6.08×10^{-11}	^{54}Mn (67)	^{55}Mn (8)	^{32}P (7)
3.82×10^9	7.26×10^7	0.464	3.30×10^{-7}	^{55}Fe (41)	^{57}Co (10)	^{53}Mn (9)	6.73×10^{-9}	^{56}Mn (45)	^{60}Co (18)	^{55}Mn (11)
4.13×10^9	2.89×10^8	0.450	6.86×10^{-7}	^{57}Fe (54)	^{61}Ni (21)	^{56}Fe (14)	4.10×10^{-7}	^{56}Mn (36)	^{52}V (12)	^{57}Mn (10)
4.41×10^9	1.30×10^9	0.442	7.57×10^{-6}	^{57}Fe (22)	^{53}Cr (14)	^{55}Mn (13)	1.74×10^{-6}	^{58}Mn (34)	^{62}Co (17)	^{64}Co (12)
7.25×10^9	9.36×10^9	0.432	9.21×10^{-3}	^{65}Ni (14)	^{59}Fe (7)	^{52}V (7)	8.45×10^{-6}	^{64}Co (22)	^{58}Mn (19)	^{54}V (13)
				25 $M_\odot$						
3.79×10^9	2.89×10^7	0.487	3.18×10^{-6}	^{53}Fe (23)	^{55}Co (20)	^{56}Ni (19)	1.53×10^{-11}	^{54}Mn (49)	^{55}Fe (17)	^{58}Co (9)
4.17×10^9	3.71×10^7	0.476	4.23×10^{-6}	^{54}Fe (21)	^{55}Co (14)	^{55}Fe (11)	8.12×10^{-10}	^{54}Mn (37)	^{58}Co (30)	^{55}Fe (8)
5.03×10^9	1.82×10^8	0.456	3.84×10^{-6}	^{56}Fe (17)	^{55}Fe (13)	^{61}Ni (10)	1.00×10^{-6}	^{56}Mn (45)	^{52}V (13)	^{60}Co (10)
5.57×10^9	5.05×10^8	0.449	1.45×10^{-5}	^{57}Fe (16)	^{56}Fe (11)	^{53}Cr (9)	7.61×10^{-6}	^{56}Mn (19)	^{58}Mn (14)	^{55}Cr (10)
7.75×10^9	2.42×10^9	0.445	1.95×10^{-3}	^{1}H (32)	^{53}Cr (9)	^{57}Fe (7)	5.17×10^{-5}	^{58}Mn (18)	^{55}Cr (13)	^{57}Mn (7)

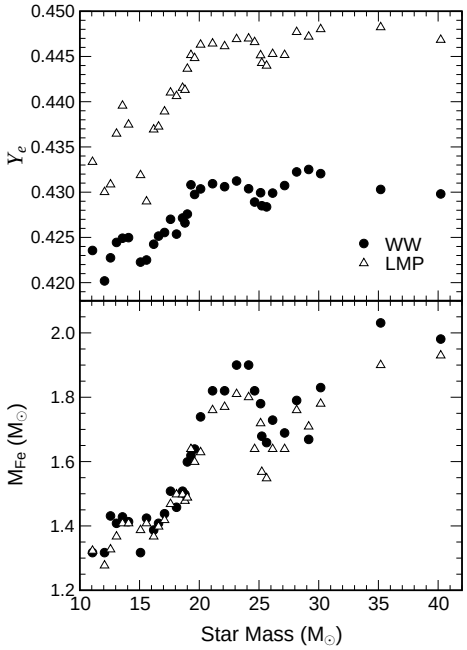

FIG. 2. Comparison of the center values of Y_e (upper part) and the iron core sizes (lower part) for 11–40 $M_\odot$ stars between the WW models and the present ones using the LMP weak interaction rates.

the other hand, mainly involves unstable manganese and cobalt isotopes. However, the lifetimes are long enough to allow for an experimental determination of the relevant GT strength distribution once radioactive ion beam facilities become operational. We finally mention that the backresonances contribute noticeably to the stellar beta decay rates for these isotopes making also measurement of the GT_+ strength on the daughter nuclei (e.g. iron and nickel isotopes) very useful.

We would like to thank G. M. Fuller for helpful discussions. This work has been partly supported by the Danish Research Council, the Carlsberg Foundation, by NATO grant CRPG973035, by the National Science Foundation (NSF-AST-9731569), by the US Department of Energy (DOE/LLNL B347885), and by the Alexander von Humboldt-Stiftung (FLF-1065004).

[1] G.M. Fuller, W.A. Fowler and M.J. Newman, Astrophys. J. Suppl. Ser. **42**, 447 (1980); Astrophys. J. Suppl. Ser. **48**, 279 (1982); Astrophys. J. **252**, 715 (1982)
[2] B.A. Brown and B.H. Wildenthal, Ann. Rev. Nucl. Part. Sci. **38**, 29 (1988)
[3] E. Caurier, computer code ANTOINE, IReS Strasbourg (1989)
[4] E. Caurier, K. Langanke, G. Martínez-Pinedo and F. Nowacki, Nucl. Phys. A **653**, 439 (1999)
[5] K. Langanke and G. Martínez-Pinedo, Nucl. Phys. A **673**, 481 (2000)
[6] S. E. Woosley and T. A. Weaver, Astrophys. J. Suppl. Ser. **101**, 181 (1995).
[7] T. Oda, M. Hino, K. Muto, M. Takahara and K. Sato, At. Data Nucl. Data Tables **56**, 231 (1994)
[8] T. Mazurek, PhD Thesis, Yeshiva Univ., (1973)
[9] C. J. Hansen, PhD Thesis, Yale Univ. (1966)
[10] M. B. Aufderheide, I. Fushiki, G. M. Fuller and T. A. Weaver, Apstrophys. J. **424**, 257 (1994).
[11] F.-K. Thielemann, K. Nomoto, and M. Hashimoto, Astrophys. J., **460**, 408, (1996)
[12] A. Heger, S.E. Woosley, G. Martínez-Pinedo and K. Langanke, in preparation